Effective Color Interpolation in CCD Color Filter Arrays Using Signal Correlation

Soo-Chang Pei, *Fellow, IEEE,* and Io-Kuong Tam

Abstract—In this paper, we propose an effective color filter array (CFA) interpolation method for digital still cameras (DSCs) using a simple image model that correlates the R, G, B channels. In this model, we define the constants K_R as green minus red and K_B as green minus blue. For real-world images, the contrasts of K_R and K_B are quite flat over a small region and this property is suitable for interpolation. The main contribution of this paper is that we propose a low-complexity interpolation method to improve the image quality. We show that the frequency response of the proposed method is better than the conventional methods. Simulation results also verify that the proposed method obtain superior image quality on typical images. The luminace channel of the proposed method outperforms 6.34-dB peak SNR over bilinear method, and the chrominace channels have a 7.69-dB peak signal-to-noise ratio improvement on average. Furthermore, the complexity of the proposed method is comparable to conventional bilinear interpolation. It requires only add and shift operations to implement.

Index Terms—Bayer pattern, color correlation, color filter array, color interpolation.

I. INTRODUCTION

DIGITAL STILL cameras (DSCs) have been widely used as image input devices. Fig. 1 shows the basic structure for a DSC. The light path divides into three sub-branches after passing through the camera lens and the optical filter. Each sub-branch corresponds to generate one of the tristimulus values of the scene. This structure requires three charged-coupled devices (CCD) to produce a color image. This is a very expensive approach and only professional DSCs use this structure. In order to reduce the cost of DSCs, digital camera designers use a single CCD, instead of using three CCDs, with a color filter array (CFA) to acquire color image [1]. Fig. 2 shows a single-CCD structure for a DSC. Since there is only one color element available in each pixel, the two missing color elements must be estimated from the adjacent pixels. This process is called CFA interpolation, or demosaicing.

The Bayer CFA pattern is the most frequently used CFA pattern, as shown in Fig. 3. Since the G (green) channel elements contribute most to luminance signals of a color image, it is reasonable to allocate higher resolution for G pixels to increase the visual quality of the image [2]. In the Bayer CFA pattern, half
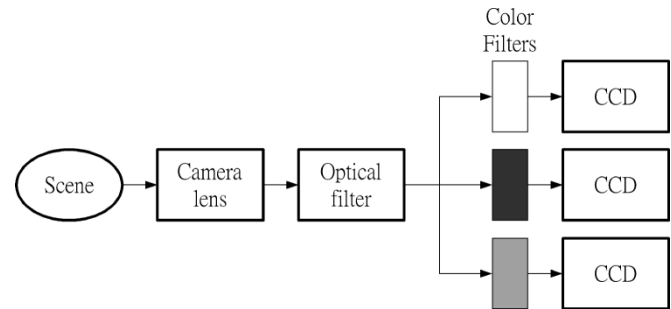
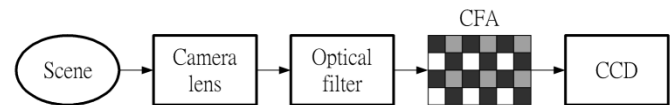Fig. 1.   Three-CCD structure for a DSC.

Fig. 2.   Single-CCD structure for a DSC.

Fig. 3.   Bayer CFA pattern.

of the pixels are assigned to the G channel, and the R (red) and B (blue) channels, which are regarded as chrominance signals, share the other half of the pixels. Since half of the pixels are assigned to the G channel, it is supposed that the G channel interpolated result will obtain superior quality than the R, B channels. For this reason, most of the R, and B channel interpolation methods are designed to make use of the G channel information. This means that if a better G channel interpolation method is adopted, not only the G channel quality will be improved, but also the R and B channels will also benefit. Therefore, the G channel quality is an important benchmark in CFA interpolation. In this paper, we focus on the development of interpolation methods for the Bayer CFA pattern.

Adams [3] provides a detailed description of conventional CFA interpolation methods and experiment results are also presented to illustrate the quality of those methods. Sakamoto and co-workers [4] provide another overview of CFA interpolation. They perform a circular zone plate (CZP) image test to study the frequency responses of the CFA interpolation methods. Hardware implementations are also provided to test the execution speed of the methods.

Bilinear interpolation is the most widely used method due to its simplicity. However, it introduces large errors in the edge region that blur the resulting image. In order to improve the visual quality in the edge region, an edge-sensing method [3] has been developed. The edge-sensing method interpolates the missing color elements according to the edge pattern of the image. However, only vertical and horizontal edges can be detected. To recover errors at diagonal edges, more complex methods must be used [3].

Kimmel [5] develops an adaptive edge-sensing method by introducing edge indicators. For a different edge pattern, the value of the edge indicators will be different. Therefore, the missing color elements can be recovered according to the edge indicators. Edge indicators can be regarded as an adaptive weighting factor. Compared with the simple edge-sensing method using a constant weighting factor, R. Kimmel's method calculates the weighing factor to adapt to the edge pattern. The quality of the interpolation result is greatly improved. However, this method is extremely complex and time consuming. It is suitable to implement by computers but not for DSCs.

The edge-sensing method is used to recover the missing G elements only, in order to recover a color image, an appropriate chrominace channel interpolation method must be developed. In this paper, we use the smooth-hue-transition method [3] in conjunction with the edge-sensing method. The smooth-hue-transition method is designed to reduce the hue artifacts by smoothing the hue value within the interpolation region. Since the human visual system is more sensitive to hue artifacts than luminance and saturation errors, the resulting image quality can be improved by reducing the hue artifacts.

Since there is a high correlation between the R, G, and B channels [6], the interpolation method using color correlation is expected to obtain better performance. Kuno and Sugiura proposed a CFA interpolation method using color correlation [7]. They assumed that the ratio of luminance signals to chrominace signals is equal to their low pass filtered ratio. A CZP image test shows that this method successfully reduces errors in vertical and horizontal directions. Hardware implementations also verify that this method received better image quality over the bilinear method. Freeman proposed a CFA interpolation method by median filtering the hue error [8]. Hue error in the edge region is greatly reduced. However, these methods [7], [8] are much more complicated than the bilinear method and this drawback must be considered.

This paper is organized as follows. Section II presents two conventional interpolation methods. In Section III, we introduce the image model, developed by Adams, Jr. [9], and the proposed method. Section IV provides CZP image test and real-world image simulation results. Section V compares the complexity of those methods described in Section II and III. Section VI provides the conclusion.

II. CONVENTIONAL INTERPOLATION METHODS

In this section, we introduce two interpolation methods that were widely used in many DSCs. The proposed method in Section III is compared with these two methods in both image quality and complexity.

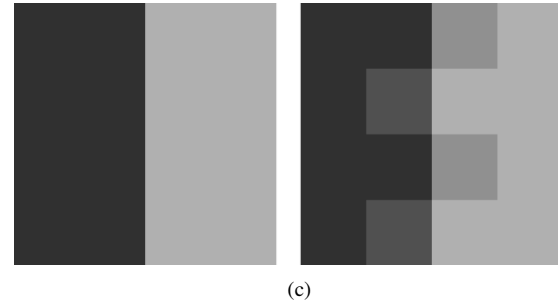Fig. 4. Reference Bayer CFA pattern.

Fig. 5. Example to illustrate the error generated by the bilinear method. (a) Edge pattern. (b) CFA pattern. (c) Original image and interpolated result.

The first approach is the use of bilinear interpolation. As shown in Fig. 4, the missing color values are interpolated using the average of the adjacent pixels.

For example

$$G'7 = \frac{G3 + G6 + G8 + G11}{4} \tag{1}$$

$$B'3 = \frac{B2 + B4}{2} \tag{2}$$

$$B'7 = \frac{B2 + B4 + B10 + B12}{4}. \tag{3}$$

Note that the locations of the R pixels and the B pixels may be interchanged, but the calculation is the same. The bilinear method ignores the edge information and does not make use of other color channels for interpolation. This method is widely used due to its simplicity; however, a large error is induced in the edge region. This error blurs the interpolated image and the quality is not satisfied.

Fig. 5 illustrates the blur error generated by the bilinear method. Assume that the original image is a vertical edge as shown in Fig. 5(a). In order to simplify the example, only two values exist in this edge pattern, where L refers to a pixel with a value less than the average value in the 3-by-3 neighborhood and H refers to a pixel with a value greater than the average value. The corresponding CFA pattern is shown in Fig. 5(b). In order to recover the vertical edge pattern, the missing G value in the middle should replace by L. By using the bilinear method,
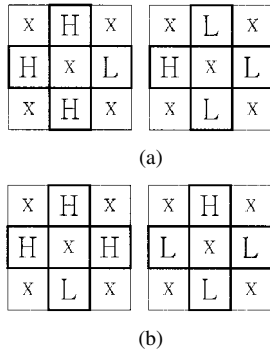
(a)

(b)

Fig. 6. (a) Vertical and (b) horizontal edge patterns.

the missing value is replaced by $G' = (L + L + L + H)/4$ and the error is equal to $\Delta G = |L - G'| = (H - L)/4$. Hence, an obvious error is produced and the edge pattern is destroyed as shown in Fig. 5(c). To overcome this drawback of the bilinear method, an edge-detection step must be used before interpolation.

Another approach is the so-called the edge-sensing interpolation. This method interpolates the missing G values according to the edge pattern of the image. To make use of the edge information, we have to study the features in the edge region. When a vertical edge is met as shown in Fig. 6(a), the horizontal gradient in a vertical edge region will be quite large. When a horizontal edge is met as shown in Fig. 6(b), the vertical gradient will be quite large. The edge-sensing method is developed based on this simple idea.

Refering to Fig. 4, one of the following three estimations for the missing $G7$ value needs to be chosen:

$$G'7H = \frac{G6 + G8}{2} \tag{4}$$

$$G'7V = \frac{G3 + G11}{2} \tag{5}$$

$$G'7A = \frac{G3 + G6 + G8 + G11}{4}. \tag{6}$$

To determine which of these three estimations is chosen, we calculate the vertical and horizontal gradients

$$\Delta H = |G6 - G8|, \Delta V = |G3 - G11|.$$

The interpolation algorithm is given by

If $(\Delta H < T)$ and $(\Delta V > T)$,
  $G'7 = G'7H$,
else if $(\Delta V < T)$ and $(\Delta H > T)$,
  $G'7 = G'7V$
else
  $G'7 = G'7A$.

where T denotes the threshold.

This method is an improvement of the bilinear interpolation. When an edge pattern is detected, interpolation is performed along the edge. The error is reduced remarkably and sharper results are obtained. However, there are two drawbacks in the edge-sensing method. First, the complexity increases significantly compared to the bilinear method. Second, this method

improves the image quality in the vertical and horizontal edges only. To recover the diagonal edge, a more complex edge-sensing method is required.

Edge-sensing interpolation is used to recover the missing G values only and we have to introduce a chrominace interpolation method to recover the R, B values. The smooth-hue-transition interpolation method is an appropriate choice here to cooperate with the edge-sensing method. The smooth-hue-transition method is an interpolation method that performs the bilinear interpolation in the hue domain. For bilinear method, interpolation is achieved by smoothing the R, G, B signals respectively. However, smooth-hue-transition interpolation can be viewed as smoothing the hue signals. To do this, a red hue value H_R and a blue hue value H_B are defined as (7).

$$H_B = \frac{B}{G}, \quad H_R = \frac{R}{G}. \tag{7}$$

As shown in Fig. 4, the missing R, B pixels can be recovered as (8) and (9).

$$B'3 = \frac{G3}{2}\left(\frac{B2}{G'2} + \frac{B4}{G'4}\right) \tag{8}$$

$$B'7 = \frac{G'7}{4}\left(\frac{B2}{G'2} + \frac{B4}{G'4} + \frac{B10}{G'10} + \frac{B12}{G'12}\right) \tag{9}$$

where $G'i$'s denote the interpolated G value.

Note that the G channel interpolation must be performed before the R, B interpolations, since this method needs the interpolated G value.

III. PROPOSED INTERPOLATION METHOD

In Section II, we introduced two well-known interpolation methods. Both use only the existing G channel neighborhood information to find the missing G values. However, there is a high correlation between the R, G, B channels. This means that interpolation of the G channel can take advantage of the R and B information. To do this, we have developed an image model exploiting the correlation between the R, G, B channels. By using the image model developed by Adams, Jr. [9], we assume that the R and B values are correlated to the G values over the extent of the interpolation pixel neighborhood. Based on this model, we define K_R as green minus red and K_B as green minus blue, as shown in (10) and (11)

$$K_R = G - R \tag{10}$$

$$K_B = G - B. \tag{11}$$

For real-world images, the contrasts of K_R and K_B are quite flat over small regions, and this property is suitable for interpolation. Fig. 7 illustrates an example of a G channel image: quite flat K_R and K_B images. In other words, instead of performing the interpolation in the G domain, we simply transform the operation into K_R or K_B domains. Based on this transformation, we reduce the interpolation error and the image quality is improved. From another viewpoint, this concept is similar to that of the smooth-hue-transition method. In our model, K_R plays the same role as H_R does in the smooth-hue-transition method. However, the complexity of the proposed method is lower since division is not required in our scheme.
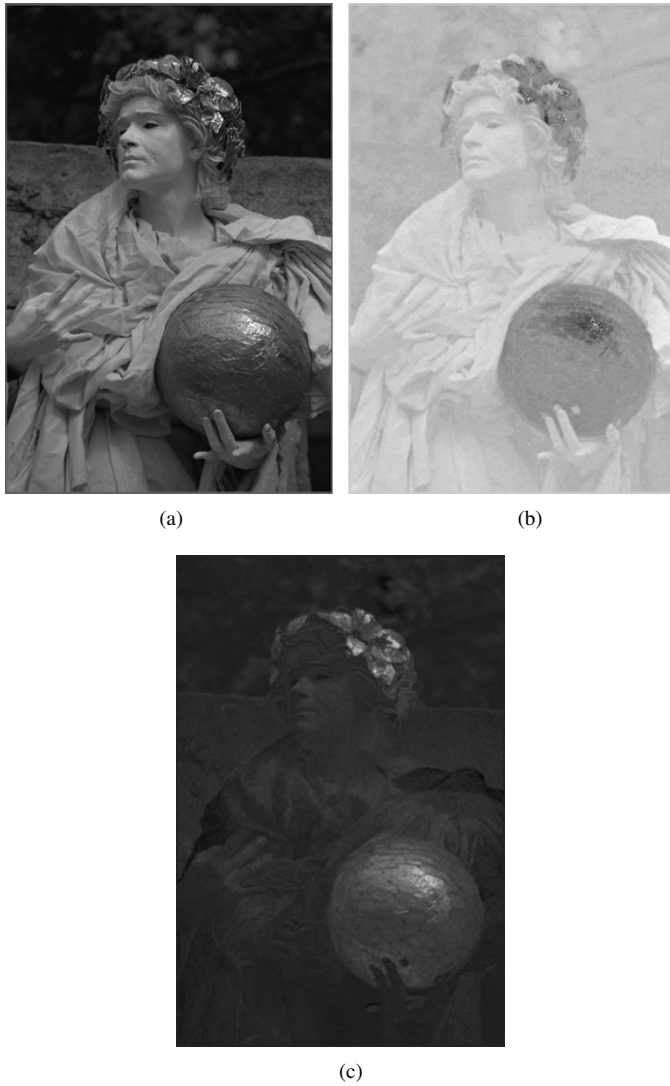
(a)   (b)

(c)

Fig. 7.   Example of (a) G channel image, (b) K_R image, and (c) K_B image.

There are three major advantages to using the K_R/K_B domain for interpolation. First, this color model is simple and has low complexity in implementation. Second, this color model is very similar to the luminance/hue/saturation color coordinate system, such as the NTSC-YIQ color system. In the development of the NTSC system, it was found possible to limit the "spatial bandwidth" of the chromatic signals (hue/saturation) without noticeable image degradation. It is because the high-frequency proportion of the chromatic signal is lower than that of the red/green/blue color signals of the nature image, and therefore the resolution of the chromatic signal can be reduced. In the K_R/K_B color model, the green channel is regarded as the luminance information, and the K_R/K_B channel can be regarded as the chromatic information (hue/saturation). The K_R and K_B channels can be viewed as the result of decorrelation between the red, green, blue channel. The high-frequency proportion of K_R and K_B is greatly reduced, and the contrasts are quite flat over small regions.

Another advantage of interpolation in the chromatic domain is that the human color vision is more sensitive to chromatic change in the low spatial frequency region than the luminance

change. According to the sinewave response measurements for colored lights obtained by van der Horst *et al.* [10], the measurements indicate that the chromatic response is shifted toward low spatial frequencies relative to the luminance response. This means that chromatic change is more noticeable to the human eye. Interpolation in the chromatic domain means that smooth the chromatic transition, which is pleasing to the human eye.

As shown in Fig. 4, to interpolate the missing G value at $R7$ pixel, we have to calculate the K_R's value around, i.e., K_R3, K_R6, K_R8, and K_R11. Since we do not have the R's value around $R7$, K_R's value can not be calculated directly. In fact, we use the estimated value of R's here. For example, we use the average of $R1$ and $R7$ to estimate $R3$, and the average of $R5$ and $R7$ to estimate $R6$, as shown in (12) and (13)

$$K_R'3 = G3 - R'3 = G3 - \frac{1}{2}(R1 + R7) \qquad (12)$$

$$K_R'6 = G6 - R'6 = G6 - \frac{1}{2}(R5 + R7). \qquad (13)$$

A. G Channel Interpolation

To find the missing G value, we have to calculate the K_R's or K_B's value around it first. Refer to Fig. 4, the missing G value at $R7$ pixel is calculated as

$$G'7 = R7 + \frac{1}{4}(K_R'3 + K_R'6 + K_R'8 + K_R'11) \qquad (14)$$

where K_R' is defined as in (12) and (13).

The interpolation of G value at a B pixel, which is performed in the K_B domain, is similar.

B. R, B Channel Interpolation

Although the design of the proposed method is focused on improving the quality of the G images, we have also developed the corresponding interpolation method for R, B channels based on the same image model. In fact, the quality of the interpolated R, B images is tremendously improved, as shown in Section IV.

Referring to Fig. 4, the proposed R, B interpolation is equivalent to a bilinear interpolation performing in the K_R or K_B domains

$$R'3 = G3 - \frac{1}{2}(K_R'1 + K_R'7) \qquad (15)$$

$$B'7 = G'7 - \frac{1}{4}(K_B'2 + K_B'4 + K_B'10 + K_B'12). \qquad (16)$$

IV. EXPERIMENT RESULTS

In this section, we present the experiment results of those interpolation methods described in Sections II and III. We do the CZP image test to evaluate the interpolation error for each frequency. Some real-world image simulations are also given. We can see that both the peak signal-to-noise ratio (PSNR) and the image visual quality are improved by using the proposed method.

A. CZP Image Test

In order to evaluate the performance of the interpolation methods for each frequency, the CZP image test is presented
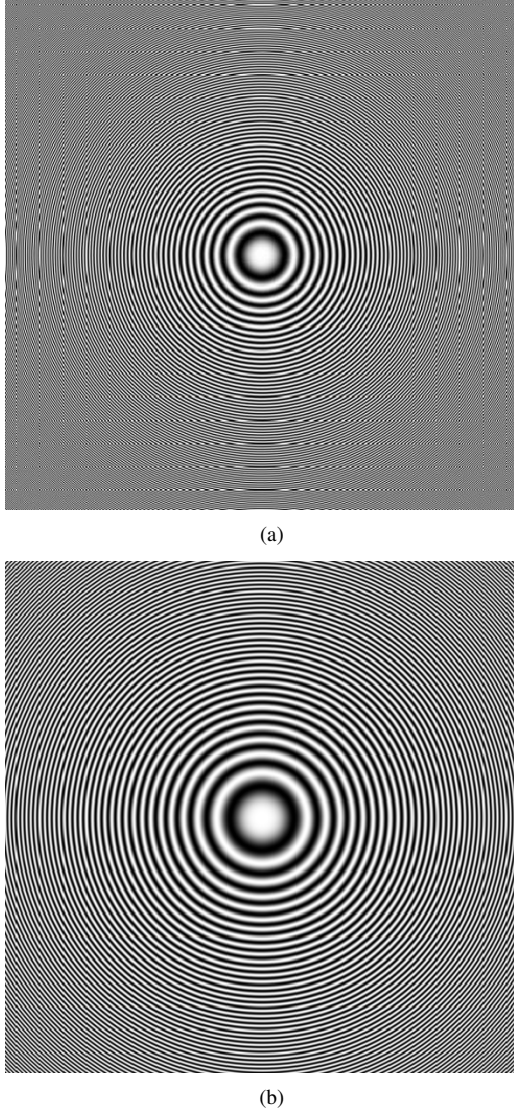
(a)

(b)

Fig. 8. CZP images with different maximal frequency. (a) $f_{\max} = N$. (b) $f_{\max} = N/2$.

here. A $N \times N$ CZP image is defined as

$$f(x,y) = C_1 \times \cos\left[\frac{\pi}{N^2}(x^2 + y^2)f_{\max}\right] + C_2 \qquad (17)$$

where C_1 and C_2 are constants.

As shown in Fig. 8, the center of the CZP is (0, 0), and the frequency at $(\pm N/2, 0), (0, \pm N/2)$ is the called the maximal frequency $f_{\max}$. The CZP defined here is more flexible than the definition in [4] because we can arbitrarily assign the value of $f_{\max}$. In our experiment, the image size is 512×512 and the maximal frequency $f_{\max}$ is $N/2$. Notice that the maximal frequency in [4] is N.

There are two reasons that we use smaller $f_{\max}$. First, the aliasing effect is reduced remarkably when using smaller $f_{\max}$ such that this effect to the interpolation result is decreased. The second reason is that we are not very concerned about the extremely high frequency.

Fig. 9 shows the horizontal interpolation error for those methods. Since the edge-sensing method is designed to recover horizontal and vertical edge errors, experiment results show
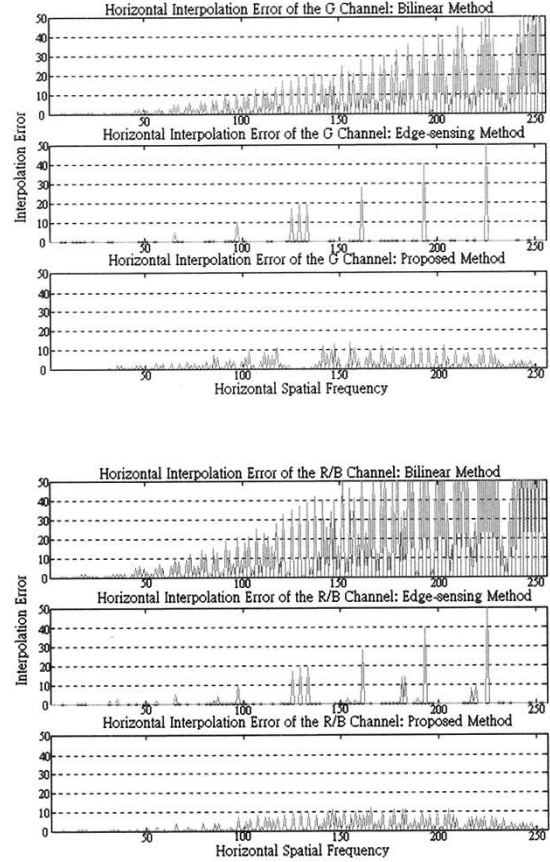

Fig. 9. Horizontal interpolation error of the R, G, B channels.

that it achieves superior results as might be expected. Note that the error of the edge-sensing method is mainly due to misdetecting the edge pattern. The performance of the proposed method is not better than the result of the edge-sensing method since the edge-detecting step is not included in the proposed scheme. However, the error is reduced remarkably compared to the bilinear method.

Fig. 10 shows the diagonal interpolation error for those methods. The error in the edge-sensing method cannot be reduced this time since the edge-sensing method cannot detect the diagonal edges. It is equal to the bilinear interpolation error at a diagonal edge region and a large error is produced. Nevertheless, the performance of the proposed method is tremendous. As will be shown in Section V, the proposed method has the capability of reducing edge error in the horizontal, vertical, and diagonal directions. This is a noticeable advantage of the proposed method that improves the image quality remarkably.

In order to observe the average performance for all directions, we average the error for all directions to produce an isotropic diagram. Fig. 11 shows the isotropic interpolation error for those methods. For low frequencies, we see that the performance of the proposed method is close to the conventional methods. When the frequency becomes higher, the advantage of the proposed method becomes more obvious.

B. Real-World Image Simulation

Here, we present some real-world image simulations to test the performance of those interpolation methods. The benchmark
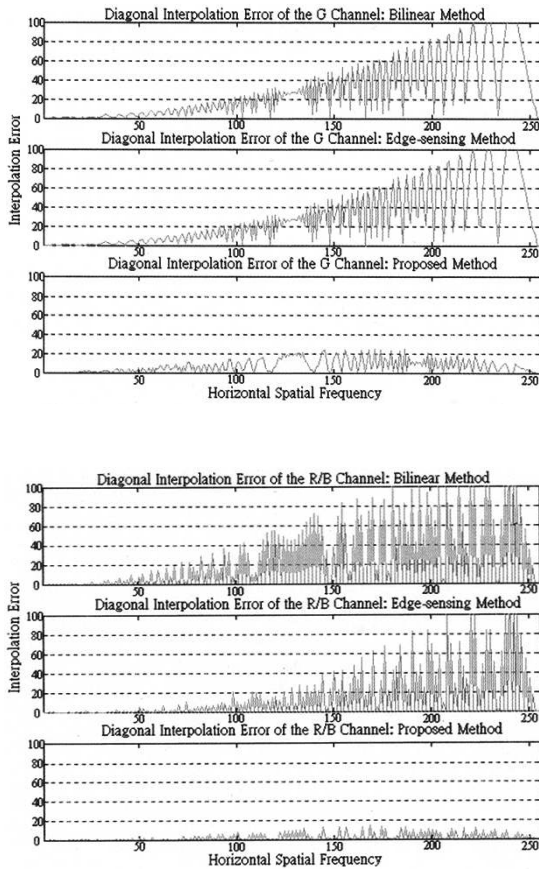
Fig. 10.   Diagonal interpolation error of the R, G, B channels.

Fig. 11.   Isotropic interpolation error of the R, G, B channels.

images used here are original and cannot be processed before by any CFA interpolation step. They can be obtained by a professional digital camera or by a color image scanner. As shown in Fig. 12, four benchmark images in the Kodak photo sampler are used in this paper. These benchmark images are sampled with Bayer CFA pattern to produce mosaic images and are then used as the input for interpolation.

In order to compare the visual quality more precisely, we magnify the interpolation result to show the details. As shown in Fig. 13, the first column is the original. Bilinear interpolation result and the edge-sensing interpolation result are placed at the second and the third column, respectively. The last column is the result of the proposed method. We see that the results of the proposed method are obviously better than the edge-sensing method, and are not distinguished from the original images. For example, the word "Bahamas" of the proposed method is even sharper. The word "SMITH" on the helmet, the word "SIX-SHOOTER" on the airplane are more obvious than the results of the edge-sensing method. Meanwhile, there are some hue changes in the feather of the parrot for both the bilinear and edge-sensing methods, but not for the proposed scheme.

Table I shows the PSNR of the interpolated images calculated using (18) and (19). The G channel of the proposed method outperforms 6.34 dB over bilinear method, and the R, B channels have 7.69-dB improvement on average. It is a great improvement over the conventional methods, and the complexity increment of the proposed method, as will be discussed in Section V, is worthwhile.
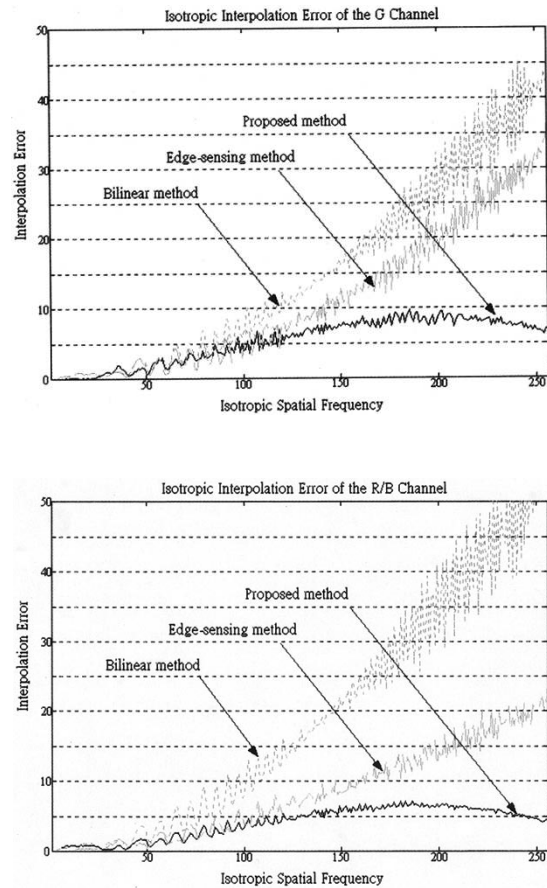
Notice that the PSNR of the edge-sensing method does not improve obviously since only the vertical and horizontal edges are recovered. The PSNR used here is defined as

$$\text{LSE} = \frac{\sum_{i=1}^{n} \sum_{j=1}^{m} (I_{ij} - I'_{ij})^2}{n \times m} \quad (18)$$

$$\text{PSNR} = 10 \log_{10}(255^2 / \text{LSE}) \quad (19)$$

where n and m are the number of the vertical and horizontal pixels, respectively. I denotes the original image and I' denotes the interpolated result.

V. DISCUSSION

In this section, a detailed investigation of the proposed method is presented. First, we compare the complexity of those interpolation methods. As we will see, the proposed method produces a better result and requires lower complexity compared to the edge-sensing method. Secondly, we prove that the image model of the proposed method is reasonable, and we show that error in the edge region can be reduced by the proposed method. Finally, we point out some problems of the edge-sensing method and the smooth-hue-transition method.

A. Complexity Comparison

There are two advantages of the proposed method. First, the image quality can be improved remarkably as shown in Section IV. Another advantage is that the complexity is acceptable

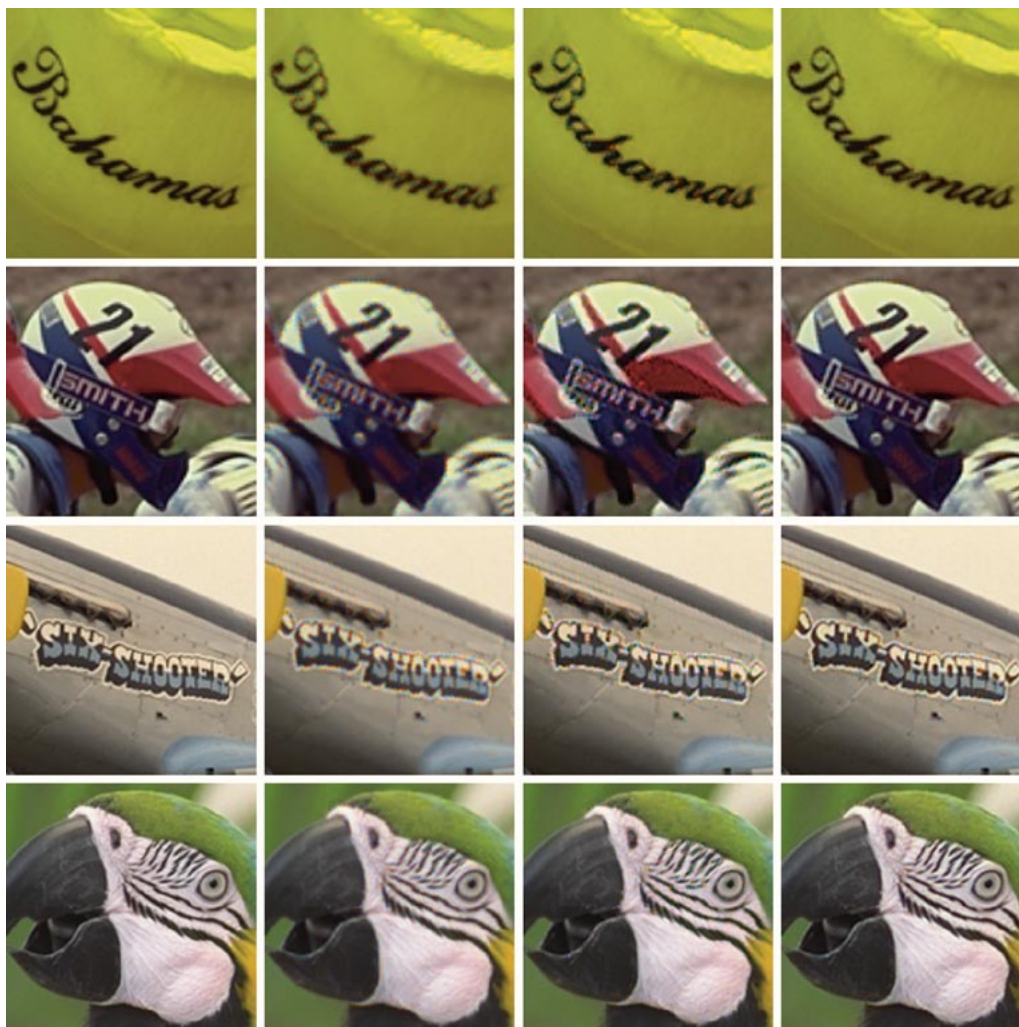Fig. 12.   Four benchmark images in Kodak photo sampler.

Fig. 13.   Detailed image of the interpolation results. The first column is the original image. The second and the third column are the result of the bilinear and edge-sensing methods, respectively. The last column is the result of the proposed method.

TABLE I
PSNR OF THE INTERPOLATED RESULTS

Image	Bilinear method			Edge-sensing method			Proposed method		
	R	G	B	R	G	B	R	G	B
cap	28.37	35.10	28.47	30.87	35.51	31.38	35.79	41.20	35.04
motor	20.74	27.23	20.66	22.68	27.51	24.23	30.11	34.76	29.72
airplane	25.75	32.48	25.42	29.54	32.95	28.82	33.82	38.41	32.69
parrot	29.57	36.11	29.20	30.92	36.33	32.92	35.89	41.90	36.63

TABLE II
COMPLEXITY COMPARISON OF BILINEAR, EDGE-SENSING, AND
THE PROPOSED METHOD

Operation	Bilinear method		Edge-sensing method		Proposed method	
	G channel	R/B channel	G channel	R/B channel	G channel	R/B channel
add	3	4	7	4	8	12
shift	1	2	3	2	3	2
Multiplication				2		
division				6		
comparison			1			
Absolute value			2			

TABLE III
MEMORY ACCESS COMPARISON OF BILINEAR, EDGE-SENSING, AND
THE PROPOSED METHOD

Operation	Bilinear method		Edge-sensing method		Proposed method	
	G channel	R/B channel	G channel	R/B channel	G channel	R/B channel
Memory read	8	12	23	28	22	28
Memory write	4	2	13	14	11	14

TABLE IV
AVERAGE 5-BY-5 BLOCK STANDARD DEVIATION OF THE BENCHMARK IMAGES

image	K_R	K_B	G channel
cap	4.02	4.66	9.55
motor	6.21	6.40	23.95
Airplane	2.23	3.67	13.09
parrot	4.51	4.42	9.56

compared with the conventional methods. Refer to Section III, the proposed method requires only add and shift operations to implement. Since multiplication and division are not required, hardware implementation is simple and the cost is reduced.

To investigate the complexity of the proposed method, we return to (14) and rewrite it as follows:

$$
\begin{aligned}
G'7 &= R7 + \frac{1}{4}(K'_R 3 + K'_R 6 + K'_R 8 + K'_R 11) \\
&= R7 + \frac{1}{4}\left[G3 - \frac{1}{2}(R7 + R1) + G6 - \frac{1}{2}(R7 + R5) \right. \\
&\quad \left. + G8 - \frac{1}{2}(R7 + R9) + G11 - \frac{1}{2}(R7 + R13) \right] \\
&= \frac{1}{2}R7 + \frac{1}{4}(G3 + G6 + G8 + G11) \\
&\quad - \frac{1}{8}(R1 + R5 + R9 + R13). \quad (20)
\end{aligned}
$$

In (20), division by 2, 4, and 8 can be implemented by a binary right-shift operation. Therefore, a total of eight additions and three shift operations are required to recover a missing G pixel in the proposed method. Similarly, we evaluate the complexity of the bilinear method, the edge-sensing method, and the proposed method. Table II shows the result of complexity comparison. The bilinear method is the simplest method. It requires only three additions and one shift operation to implement the G channel interpolator. The proposed method almost triples the complexity of it, but this complexity increment is worthwhile in order to improve the image quality. Fewer addition operations are required in the edge-sensing method compared to the proposed method. However, the edge-sensing method needs comparison and absolute value operation to detect edge patterns, and divisions and multiplications are needed to calculate the missing R and B pixels. The complexity increment is obviously greater, and image quality improvement is less than the proposed method. This indicates that the proposed method is a

better choice than edge-sensing method in both complexity and image quality considerations.

Today, most digital cameras are implemented with a general purpose digital signal processor (DSP), and the memory access frequency has a great effect to the performance of an algorithm. When a memory access is needed, the DSP has to stop and wait for the data. Therefore, the execution time of an algorithm is directly proportion to the number of memory access. Refering to (20), the proposed method required eight addition and three shift operation. If we assume that each addition takes two data, and each shift operation takes one, it means that the proposed method needs 8×2 memory read accesses and 8×1 memory write accesses for eight additions, and 3×2 memory read and write accesses for three shift operations. Based on the same rule, we can evaluate the required number of memory access of the bilinear method, the edge-sensing method, and the proposed method as Table III.

According to Table III, the proposed method requires triple the number of memory access compared with the bilinear method, and therefore the execution time of the proposed method is triple the time of the bilinear method. Since the execution cycles required by multiplication and division are the same as addition and shift operation, the execution time of the edge-sensing method is close to the proposed method. However, most of the system-on-chip (SOC) requires hardware acceleration to increase performance. The hardware implementation complexity of the proposed method is lower because only addition and shift operation are required.

B. Advantages of the Proposed Method

Here, we explain why the proposed method works better. As mentioned before, the proposed method can be viewed as a bilinear interpolation in the K_R and K_B domains. For real-world images, the contrasts of K_R and K_B are quite flat over a small region and thus this property is suitable for interpolation. Fig. 7 is an example to illustrate that K_R and K_B satisfy this assumption. In order to show that this assumption is correct, we calculate the average standard deviation (STD) of K_R, K_B, and the G channel with block size 5-by-5, as shown in Table IV. We see that the STD of K_R and K_B are smaller than the STD of the G channel, and this is an advantage for interpolation.
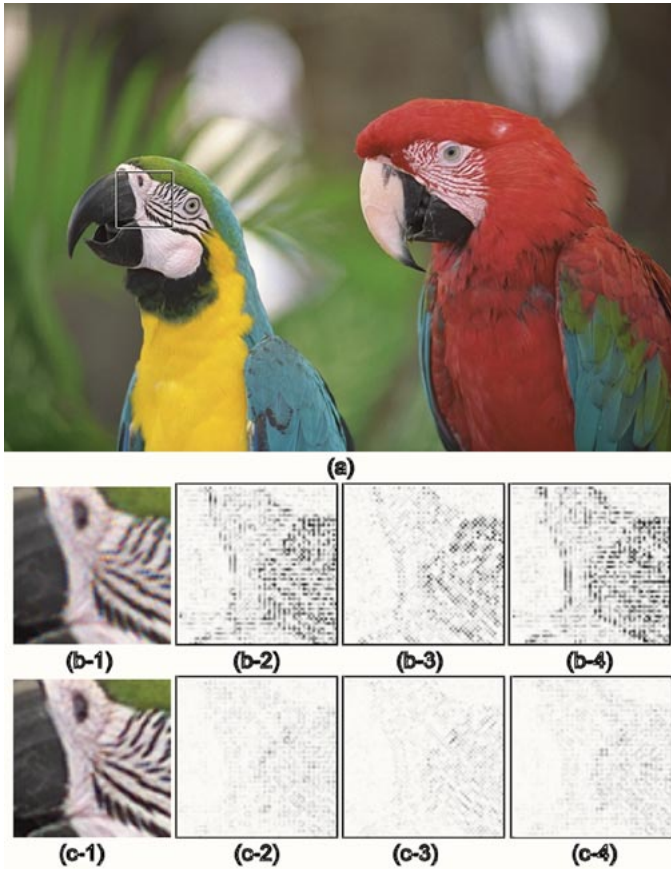
Fig. 14. (a) Original parrot image and magnified eye square region, (b-1)–(b-4) and (c-1)–(c-4) show the interpolated images and R, G, B channel errors of the parrot eye image using bilinear interpolation and the proposed method, respectively.
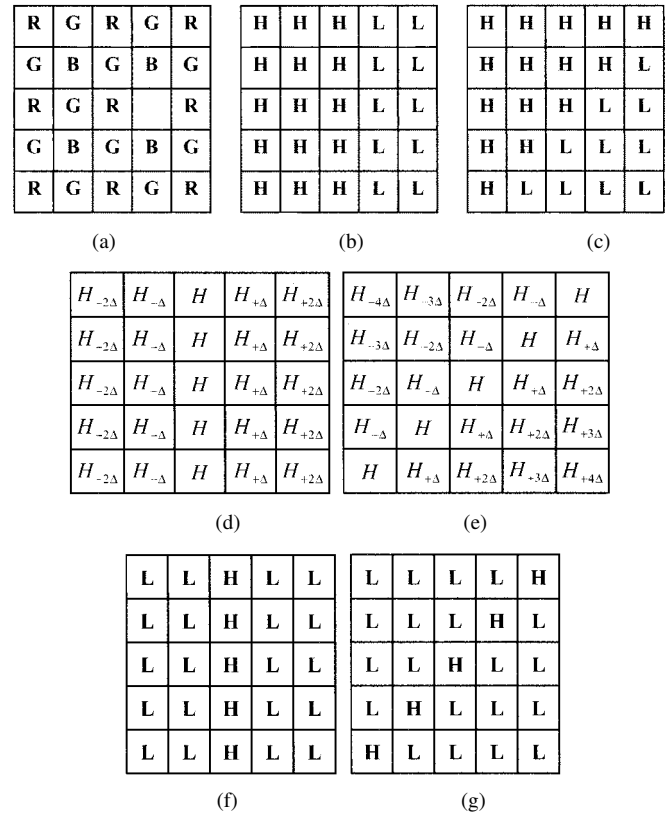

Fig. 15. Reference Bayer CFA and the step/ramp/roof edge patterns. (a) CFA pattern. (b) Vertical step edge. (c) Diagonal step edge. (d) Vertical ramp edge. (e) Diagonal ramp edge. (f) Vertical roof edge. (g) Diagonal roof edge. (Note: $H_{\pm k\Delta}$ in the ramp edge indicates the value of $H \pm k\Delta$.)

Another advantage of the proposed method is that the error in the edge region is reduced. Fig. 14 shows the edge error comparison between the results of bilinear interpolation, and the proposed method. Fig. 14(a) indicates the interpolated region with the lowest PSNR. The interpolated image, and the red, green, blue errors of the bilinear method is magnified and is shown in Fig. 14(b-1)–(b-4), respectively. The same result of the proposed method is shown in Fig. 14(c-1)–(c-4). As we can see, most of the bilinear interpolation error is located at the edge. Therefore, interpolation quality will be improved greatly if error at the edge is reduced. Fig. 14(c-1)–(c-4) shows that the proposed method can reduce the edge error effectively.

Here, we give an example to illustrate that the proposed method can reduce error at the edge. The reference CFA pattern is shown as in Fig. 15(a). Fig. 15(b) and (c), (d) and (e), and (f) and (g), respectively, show the vertical and diagonal edge patterns of step edge, ramp edge, and the roof edge. At this time, we assume that all R, G, B channels satisfy this edge pattern. By using the bilinear method, the missing G value at the middle of the vertical step edge is calculated as follows:

$$G'_B = \frac{1}{4}(H_G + H_G + H_G + L_G) = \frac{3}{4}H_G + \frac{1}{4}L_G \quad (21)$$

where H_G and L_G denote the G values located at the H and L positions, respectively. The interpolation error using bilinear method is

$$\Delta G_B = H_G - G'_B = \frac{1}{4}(H_G - L_G). \quad (22)$$

By using the edge-sensing method, the missing G value at the middle is calculated as follows:

$$G'_E = \frac{1}{2}(H_G + H_G) = H_G, \quad \Delta G_E = 0. \quad (23)$$

The interpolation error is zero, because the edge-sensing method can recover vertical and horizontal edge perfectly.

By using the proposed method, the missing G value can be calculated according to (20) as follows:

$$\begin{aligned} G'_P &= H_R + \frac{1}{4}\left[H_G - \frac{1}{2}(H_R + H_R) + H_G - \frac{1}{2}(H_R + H_R)\right.\\ &\quad \left. + H_G - \frac{1}{2}(H_R + H_R) + L_G - \frac{1}{2}(H_R + L_R)\right] \\ &= H_R + \frac{1}{4}\left[3(H_G - H_R) + \left[L_G - \frac{1}{2}(H_R + L_R)\right]\right] \\ &= \frac{3}{4}H_G + \frac{1}{4}L_G + \frac{1}{8}(H_R - L_R) \end{aligned} \quad (24)$$

where H_R and L_R denote the R values located at the H position and L position respectively. The interpolation error using the proposed method is

$$\Delta G_P = H_G - G'_P = \frac{1}{4}(H_G - L_G) - \frac{1}{8}(H_R - L_R). \quad (25)$$

Edge	Direction	Bilinear method	Edge-sensing method	Proposed method
Step	Vertical	$(H_G - L_G)/4$	0	$(H_G - L_G)/8$
Step	Diagonal	$(H_G - L_G)/2$	$(H_G - L_G)/2$	$(H_G - L_G)/4$
Ramp	Vertical	0	0	0
Ramp	Diagonal	0	0	0
Roof	Vertical	$\Delta/2$	0	$\Delta/4$
Roof	Diagonal	Δ	Δ	$\Delta/2$

Assume that $H_{K_R} = H_G - H_R$ and $L_{K_R} = L_G - L_R$ denote the K_R values located at the H position and L position respectively. Equation (24) can be rewritten as follows:

$$\Delta G_P = H_G - G'_P = \frac{1}{4}(H_G - L_G) - \frac{1}{8}(H_R - L_R)$$
$$= \frac{1}{8}(H_G - L_G) + \frac{1}{8}(H_{K_R} - L_{K_R}). \quad (26)$$

Refering to Table III, we see that the STD of K_R and K_B are smaller than the STD of the G channel. This means that the difference between H_{K_R} and L_{K_R} is typically smaller than the difference between H_G and L_G, i.e., $H_G - L_G > H_{K_R} - L_{K_R}$

$$\Delta G_P = \frac{1}{8}(H_G - L_G) + \frac{1}{8}(H_{K_R} - L_{K_R})$$
$$< \frac{1}{4}(H_G - L_G) = \Delta G_B. \quad (27)$$

If we assume that the values of K_R are perfectly match to the image model introduced in Section III, we have $H_{K_R} \approx L_{K_R} = $ constant. Therefore, (26) can be simplified as

$$\Delta G_P = \frac{1}{8}(H_G - L_G) + \frac{1}{8}(H_{K_R} - L_{K_R})$$
$$\approx \frac{1}{8}(H_G - L_G) = \frac{1}{2}\Delta G_B. \quad (28)$$

The assumption $H_{K_R} \approx L_{K_R} = $ constant means that the color differences K_R and K_B are remain constant across the edge, only the luminance G is changed. Therefore, the edge error of the proposed method are minimized based on color differences invariant assumption. Compare this interpolation error to the result of bilinear method, we found that half of the error is reduced. Similarly, we study the error at diagonal edge as shown in Fig. 15(c). By using the bilinear method, we have

$$G'_B = \frac{1}{4}(H_G + H_G + L_G + L_G) = \frac{1}{2}H_G + \frac{1}{2}L_G \quad (29)$$
$$\Delta G_B = H_G - G'_B = \frac{1}{2}(H_G - L_G). \quad (30)$$

By using the edge-sensing method, the result is identical to that of bilinear interpolation. It is because the edge-sensing method cannot recover diagonal edge

$$G'_E = \frac{1}{2}(H_G + L_G), \quad \Delta G_E = \frac{1}{2}(H_G + L_G). \quad (31)$$

By using the proposed method, the error is reduced as follows:

$$G'_P = \frac{1}{2}(H_G + L_G) + \frac{1}{4}(H_R - L_R) \quad (32)$$
$$\Delta G_P = H_G - G'_P = \frac{1}{2}(H_G - L_G)$$
$$- \frac{1}{4}(H_R - L_R) \approx \frac{1}{4}(H_G - L_G) = \frac{1}{2}\Delta G_B. \quad (33)$$

Table V shows the edge error by using bilinear interpolation, the edge-sensing interpolation, and the proposed method. Note that the edge error results of the proposed method are derived based on the color differences invariant assumption. The edge-sensing method can recover vertical and horizontal edge perfectly; however, the performance in the diagonal direction is the same as bilinear interpolation.

VI. CONCLUSION

A new CFA interpolation method is proposed in this paper. The frequency response of the proposed method is better than the conventional methods, especially at high frequency. Real-world image simulation also shows that the proposed method produces superior PSNR and better image quality performance. The luminace channel of the proposed method outperforms 6.34 dB over the bilinear method, and the chrominace channels have 7.69-dB improvement, on average, on typical images. Furthermore, the complexity of the proposed method is acceptable, as add and shift operations are required.

REFERENCES

[1] J. Adams, K. Parsulski, and K. Spaulding, "Color processing in digital cameras," *IEEE Micro*, pp. 20–29, Nov.–Dec. 1998.
[2] W. B. Pennebaker and J. L. Mitchell, *JPEG Still Image Data Compression Standard*. New York: Van Nostrand Reinhold, 1993.
[3] J. E. Adams Jr., "Interactions between color plane interpolation and other image processing functions in electronic photography," in *Proc. SPIE*, vol. 2416, C. Anagnostopoulos and M. Lesser, Eds., Bellingham, WA, 1995, pp. 144–151.
[4] T. Sakamoto, C. Nakanishi, and T. Hase, "Software pixel interpolation for digital still cameras suitable for a 32-Bit MCU," *IEEE Trans. Consumer Electron.*, vol. 44, pp. 1342–1352, Nov. 1998.
[5] R. Kimmel, "Demosaicing: Image reconstruction from color CCD samples," *IEEE Trans. Image Processing*, vol. 8, pp. 1221–1228, Sept. 1999.
[6] W. K. Pratt, *Digital Image Processing*, 3rd ed. New York, NY: Wiley, 2001.
[7] T. Kuno and H. Sugiura, "New interpolation method using discriminated color correlation for digital still cameras," *IEEE Trans. Consumer Electron.*, vol. 45, no. 1, pp. 259–267, Feb. 1999.
[8] W. T. Freeman, "Median Filter for Reconstructing Missing Color Samples,", Feb. 1988. U.S. patent 4 724 295.
[9] J. E. Adams Jr., "Design of practical color filter array interpolation algorithm for digital still cameras," in *Proc. SPIE*, vol. 3028, D. Sinha, Ed., Bellingham, WA, 1997, pp. 117–125.
[10] C. J. C. van der Horst, C. M. de Weert, and M. A. Bouman, "Transfer of spatial chromaticity—Contrast at threshold in the human eye," *J. Opt. Soc. Amer.*, vol. 57, no. 10, pp. 1260–1266, Oct. 1967.

Soo-Chang Pei (F'00) was born in Soo-Auo, Taiwan in 1949. He received B.S.E.E. degree from National Taiwan University (NTU), Taipei, Taiwan, R.O.C., in 1970 and the M.S.E.E. and Ph.D. degrees from the University of California, Santa Barbara (UCSB), in 1972 and 1975, respectively.

He was an engineering officer in the Chinese Navy Shipyard from 1970 to 1971. From 1971 to 1975, he was a Research Assistant at UCSB. He was a Professor and Chairman in the Electrical Engineering Department, Tatung Institute of Technology, from 1981 to 1983, and at NTU from 1995 to 1998 . Presently, he is a Professor in the Electrical Engineering Department at NTU. His research interests include digital signal processing, image processing, optical information processing, and laser holography.

Dr. Pei received the National Sun Yet-Sen Academic Achievement Award in Engineering in 1984, the Distinguished Research Award from the National Science Council, R.O.C., from 1990 to 1998, the Outstanding Electrical Engineering Professor Award from the Chinese Institute of Electrical Engineering in 1998, the Academic Achievement Award in Engineering from the Ministry of Education in 1998, the IEEE Fellow in 2000 for contributions to the development of digital eigenfilter design, color image coding and signal compression, and electrical engineering education in Taiwan, the Pan Wen-Yuan Distinguished Research Award in 2002, and the National Chair Professor Award from the Ministry of Education in 2002. He was President of the Chinese Image Processing and Pattern Recognition Society in Taiwan from 1996–1998, and is a member of Eta Kappa Nu and the Optical Society of America.

Io-Kuong Tam received the B.S. and M.S. degrees from National Taiwan University, Taipei, Taiwan, R.O.C., in 1998 and 2000, respectively.

He is currently an Engineer with the Realtek Semiconductor Corporation, Hsinchu, Taiwan, R.O.C. His research interests include image interpolation, watermarking, and image compression.